

# Metal-free photocatalytic cross-electrophile coupling enables C1 homologation and alkylation of carboxylic acids with aldehydes

Received: 24 November 2023

Accepted: 5 February 2024

Published online: 19 February 2024

Check for updates

Stefano Bonciolini<sup>1,7</sup>, Antonio Pulcinella<sup>1,7</sup>, Matteo Leone <sup>1,2</sup>, Debora Schirolì<sup>1,3</sup>, Adrián Luguera Ruiz <sup>1,4</sup>, Andrea Sorato <sup>1</sup>, Maryne A. J. Dubois<sup>5</sup>, Ranganath Gopalakrishnan <sup>5</sup>, Geraldine Masson <sup>2</sup>, Nicola Della Ca' <sup>3</sup>, Stefano Protti <sup>4</sup>, Maurizio Fagnoni <sup>4</sup>, Eli Zysman-Colman <sup>6</sup>, Magnus Johansson <sup>5</sup> & Timothy Noël <sup>1</sup> ✉

In contemporary drug discovery, enhancing the  $sp^3$ -hybridized character of molecular structures is paramount, necessitating innovative synthetic methods. Herein, we introduce a deoxygenative cross-electrophile coupling technique that pairs easily accessible carboxylic acid-derived redox-active esters with aldehyde sulfonyl hydrazones, employing Eosin Y as an organophotocatalyst under visible light irradiation. This approach serves as a versatile, metal-free  $C(sp^3)-C(sp^3)$  cross-coupling platform. We demonstrate its synthetic value as a safer, broadly applicable C1 homologation of carboxylic acids, offering an alternative to the traditional Arndt-Eistert reaction. Additionally, our method provides direct access to cyclic and acyclic  $\beta$ -arylethylamines using diverse aldehyde-derived sulfonyl hydrazones. Notably, the methodology proves to be compatible with the late-stage functionalization of peptides on solid-phase, streamlining the modification of intricate peptides without the need for exhaustive *de-novo* synthesis.

In drug discovery, the 3D structure of proteins is crucial for the success of drugs. The increased use of  $sp^3$ -hybridized carbon atoms ( $F_{sp^3}$ ) is key, as it correlates with a drug's effectiveness and safety<sup>1</sup>. This trend, known as 'Escape from Flatland'<sup>2</sup>, involves increasing  $F_{sp^3}$  in drugs for better alignment with protein structures, enhancing selectivity and efficacy<sup>3</sup>. This strategy improves target interaction and reduces side effects, balancing effective treatment with minimal negative effects.

Historically, classical cross-coupling reactions have been a linchpin in synthetic chemistry, enabling the straightforward construction of  $C(sp^2)-C(sp^2)$  bonds and thereby propelling the production of

planar, biaryl structures. This entrenched reliance on cross-coupling has inadvertently sculpted a discernible bias in small molecule drug design, steering the generation of libraries that predominantly feature structurally analogous, two-dimensional compounds<sup>4</sup>. While there have been laudable strides made within the domain of  $C(sp^3)-C(sp^3)$  cross-coupling, contemporary methodologies are oftentimes plagued by several pragmatic limitations<sup>5,6</sup>. They typically necessitate sizable excesses of one coupling partner and frequently hinge upon non-abundant starting materials, such as air- and moisture-sensitive alkyl organometallics, thereby constraining the reaction scope and

<sup>1</sup>Flow Chemistry Group, Van't Hoff Institute for Molecular Sciences (HIMS), University of Amsterdam, Science Park 904, 1098 XH Amsterdam, The Netherlands. <sup>2</sup>Institut de Chimie des Substances Naturelles, CNRS, Univ. Paris-Saclay, 1 Avenue de la Terrasse, 91198 Gif-sur-Yvette, Cedex, France. <sup>3</sup>SynCat Lab, Department of Chemistry, Life Sciences and Environmental Sustainability, University of Parma, 43124 Parma, Italy. <sup>4</sup>PhotoGreen Lab, Department of Chemistry, University of Pavia, 27100 Pavia, Italy. <sup>5</sup>Medicinal Chemistry, Research and Early Development, Cardiovascular, Renal and Metabolism (CVRM), BioPharmaceuticals R&D, AstraZeneca, Gothenburg, Sweden. <sup>6</sup>Organic Semiconductor Centre, EaStCHEM School of Chemistry, Purdie Building, North Haugh University of St Andrews, St Andrews, Fife KY16 9ST, UK. <sup>7</sup>These authors contributed equally: Stefano Bonciolini, Antonio Pulcinella.

✉ e-mail: [t.noel@uva.nl](mailto:t.noel@uva.nl)



bases, strongly limiting the substrate scope of the transformation and its scalability<sup>40,41</sup>. For seminal radical variants, Barton proposed a photoinduced C1 homologation of *N*-hydroxy-2-thiopyridone esters, although this strategy suffered from low functional group compatibility, a narrow scope, and requisite lengthy synthetic sequences<sup>42,43</sup>. In this context, we present the utilization of ethyl glyoxalate-derived sulfonyl hydrazone **2a** as a bench-stable and easy-to-handle crystalline radical acceptor to realize the C1 homologation of carboxylic acids under mild conditions (Fig. 1D). As a subsequent, potent application of this synthetic paradigm, our attention was drawn by the synthesis of  $\beta$ -arylethylamines, a prevalent structural motif within numerous drugs and natural products<sup>44</sup>. Although various synthetic routes have been delineated, an intuitive retrosynthetic strategy entailing a cross-coupling reaction between a benzyl electrophile and  $\alpha$ -amino nucleophile has remained underrepresented<sup>44–46</sup>. We posit that the advanced cross-electrophile coupling between NHPI esters and aldehyde sulfonyl hydrazones will provide a straightforward and direct route for the efficient preparation of substituted cyclic and acyclic  $\beta$ -arylethylamines (Fig. 1E). Concluding with a third robust synthetic application of this strategy, the methodology demonstrates significant utility in the late-stage functionalization (LSF) of peptides on solid-phase, enabling the modification of complex peptides under mild conditions and obviating the need for tedious de-novo synthesis (Fig. 1F)<sup>47–49</sup>.

## Results

### Reaction optimization

We initially commenced to develop a direct decarboxylative C1 homologation, beginning with *N*-Boc (*L*)-Proline, but we were met with

failure to produce the desired product **3** (see Supplementary Information, Section 5.1). This result was linked to the noted sensitivity of aldehyde sulfonyl hydrazones to bases, which are indispensable to promote the decarboxylation process<sup>21,50</sup>. Consequently, our investigation focused on the use of well-established *N*-(acyloxy)phthalimides (NHPI-based esters) as redox-active esters (RAEs) in an effort to sidestep the necessity for bases during the decarboxylative generation of nucleophilic carbon radicals. An exhaustive screening of all reaction parameters (see Supplementary Information, Section 5.2) led us to discover that the targeted homologated product **3** could be obtained in excellent yields (Table 1, Entry 1, 90% yield) when a dichloromethane (0.1 M) solution composed of ethyl glyoxalate-derived 4-trifluoromethyl-phenyl sulfonyl hydrazone **2a** (1.0 equiv.) as the radical acceptor, *N*-Boc (*L*)-Proline RAE **1a** (1.0 equiv.) as the radical precursor, Hantzsch ester (HE, 1.5 equiv.) as the reductive quencher, and disodium Eosin Y (EYNa<sub>2</sub>, 10 mol%) as the photocatalyst was irradiated with blue LEDs (40 W Kessil, 456 nm, PRI60L) for 12 h. The yield reflects the one obtained for the final product **3**, achieved when the hydrazinyl intermediate was swiftly subjected to cleavage conditions in ethanol, according to our previous report<sup>27</sup>. Evaluating a two-step one-pot procedure, with trifluorotoluene as the solvent, revealed diminished yields of **3** (Table 1, Entry 2). Surprisingly, an excess of radical acceptor **2a** did not markedly influence the reactivity (Table 1, Entry 3). Noteworthy is the underperformance of more expensive organophotoredox catalysts like 4CzIPN, 3DPA<sub>2</sub>FBN or the widely-used transition-metal based photocatalyst Ru(bpy)<sub>3</sub>PF<sub>6</sub> (Table 1, Entries 4–6)<sup>51,52</sup>. HE played a major role in the transformation, as other reductive quenchers, such as DABCO, DIPEA, or tetramethylguanidine entirely inhibited the reaction (see Supplementary Table 5).

**Table 1 | Optimization of the photochemical step for the C1 homologation of RAE 1a**

| Entry | Deviation   | Yield of <b>3</b> <sup>a</sup> |
|-------|---|--------------------------------|
| 1     | None  | 90%                            |
| 2     | Trifluorotoluene as solvent   | 60%                            |
| 3     | 2 equiv. <b>2a</b>  | 81%                            |
| 4     | 4CzIPN 5 mol% as PC   | 61%                            |
| 5     | 3DPA <sub>2</sub> FBN 5 mol% as PC                                  | 53%                            |
| 6     | [Ru(bpy) <sub>3</sub> ](PF <sub>6</sub> ) <sub>2</sub> 1 mol% as PC | 66%                            |
| 7     | No EYNa <sub>2</sub>  | n.d.                           |
| 8     | No EYNa <sub>2</sub> , 390 nm                                       | 40%                            |
| 9     | Dark  | n.d.                           |

<sup>a</sup>Yields were determined by <sup>1</sup>H NMR using trichloroethylene as external standard (0.2 mmol scale, 0.1 M). See Supplementary Information for experimental details.

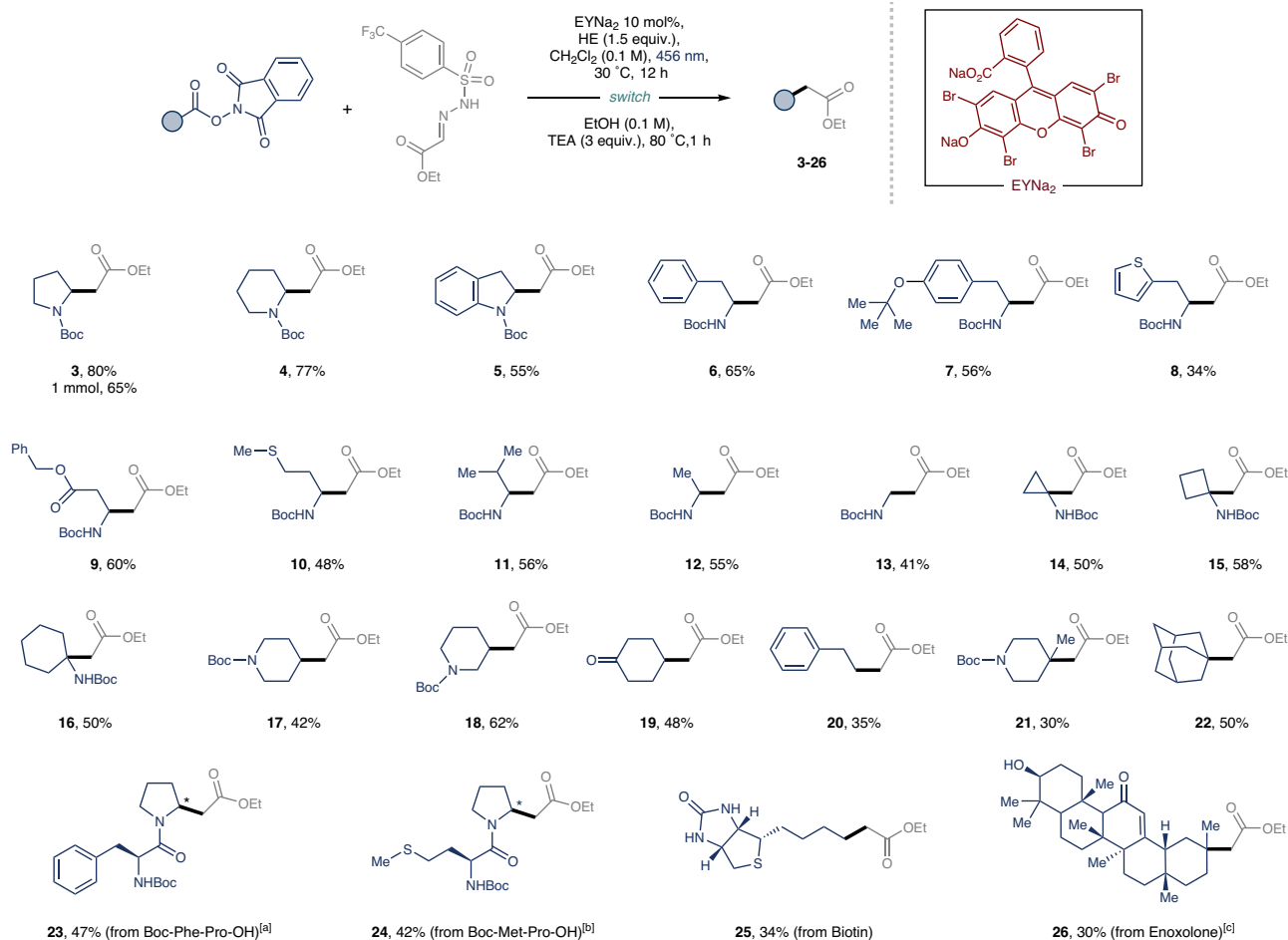


**Fig. 2 | Scope of the C1 homologation.** Coupling of carboxylic acid-derived redox-active esters (RAEs) with ethyl glyoxylate-derived 4-(trifluoromethyl)phenyl sulfonyl hydrazones **2a**. Reaction conditions: redox active ester (0.3 mmol, 1 equiv.), **2a** (1

equiv.), Hantzsch ester (1.5 equiv.) and EYNa<sub>2</sub> (0.10 equiv.) in 3 mL of CH<sub>2</sub>Cl<sub>2</sub> (0.1 M). For further experimental details see the Supplementary Information. [a] >20:1 d.r. [b] 3:1 d.r. [c] 2.5:1 d.r.

Remarkably, incorporating acidic additives, such as HFIP, TFA, and various amino acids, did not substantially impact the reactivity (see Supplementary Tables 3 and 8). Control experiments conducted to explore the formation of donor-acceptor complexes between RAE **1a** and HE, performed at 456 and 390 nm without EYNa<sub>2</sub>, either yielded no product or achieved lower yields (Table 1, Entries 7–8), underscoring the crucial role of the photocatalyst in photoinitiating the reaction, thus securing higher yields<sup>53,54</sup>. Running the reaction in the dark resulted in the quantitative recovery of all starting materials (Table 1, Entry 9). Notably, applying the optimized conditions to the less electrophilic 4-CF<sub>3</sub>-benzaldehyde-derived sulfonyl hydrazone **2c** as the radical acceptor yielded the corresponding  $\beta$ -arylethylamine product **46** in a 58% NMR yield. Additional screening of reaction parameters did not produce any enhancements in yield (see Supplementary Information, Section 5.3).

### C1 homologation substrate scope

Having established optimal reaction conditions, we next investigated the scope of the photochemical C1 homologation of RAEs derived from readily available carboxylic acids (Fig. 2). As expected, *N*-Boc protected cyclic amino acids afforded the desired products (**3–5**) in good yields. Moreover, linear proteogenic amino acids underwent homologation to the respective ethyl esters (**6–13**) under the standardized reaction conditions. Noteworthy is the performance of challenging substrates, such as the redox-sensitive methionine and thiophene-derived amino acid, which, despite providing the target

compounds (**8** and **10**), did so in somewhat attenuated yields. The protocol's generality was highlighted through the homologation of sterically hindered cyclic tertiary amino acids, producing the target products in synthetically useful yields (**14–16**). A subsequent examination of various inactivated primary, secondary, and tertiary RAEs revealed that all coupled with glyoxalate-derived sulfonyl hydrazones **2a**, presenting moderate to good yields (**17–22**). In a particularly notable development, two dipeptides underwent photochemical homologation, yielding the targeted homoproline analogues (**23–24**)<sup>55</sup>. Importantly, the mild conditions of this photocatalytic C1 homologation protocol facilitated the conversion of natural products like biotin and enoxolone—each harboring different sensitive functional groups—to their corresponding ethyl esters (**25–26**), not accessible by the aforementioned methods.

### Alkylation substrate scope

We next aimed to explore further the generality of our developed reaction conditions, applying them to the cross-electrophile coupling of RAEs, derived from a diverse set of carboxylic acids, with various aldehyde-derived sulfonyl hydrazones (Fig. 3). We envisioned providing streamlined access to cyclic and acyclic  $\beta$ -arylethylamines, thereby presenting a new, intuitive radical disconnection for practitioners in the field<sup>44</sup>. Regarding the scope of the  $\alpha$ -amino RAEs, a myriad of medicinally pertinent cyclic structures—encompassing azetidines, piperazines, indolines, and isoquinolines—were successfully coupled, achieving synthetically useful yields in all cases (**27–33**)<sup>56</sup>.

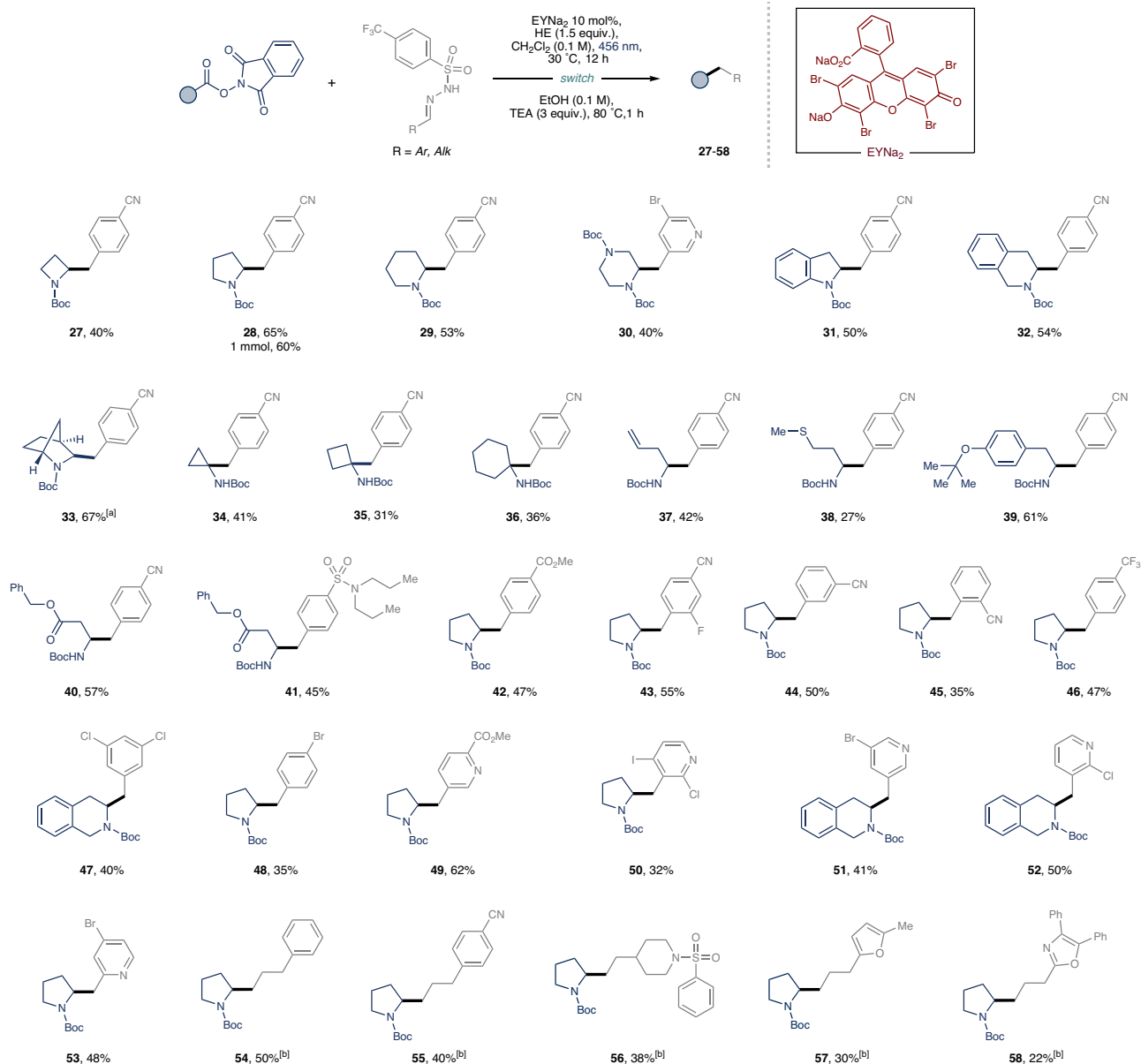


**Fig. 3 | Scope of the alkylation.** Cross-electrophile coupling of RAEs with aromatic and aliphatic aldehyde-derived sulfonyl hydrazones. Reaction conditions: RAE (0.3 mmol, 1 equiv.), Sulfonyl Hydrazone (1 equiv.), Hantzsch ester (1.5 equiv.) and

EYNa<sub>2</sub> (0.10 equiv.) in 3 mL of CH<sub>2</sub>Cl<sub>2</sub> (0.1 M). For further experimental details see the Supplementary Information. [a] 1:1.4 d.r. [b] 2 equiv. of N-Boc (L)-Proline RAE **1a** was used.

Significantly, the methodology enabled the conversion of even challenging tertiary RAEs, facilitating the creation of quaternary centers, albeit with somewhat reduced yields (**34–36**). Beyond cyclic structures, the protocol also exhibited proficiency with a range of linear amino acids, yielding the corresponding  $\beta$ -arylethylamines in moderate to good isolated yields (**37–41**). An assessment of the sulfonyl hydrazones scope indicated optimal performance with electron-poor groups (see Supplementary Information, Section 11). Noteworthy, the metal-free nature of the protocol tolerated halogenated arenes and heterocycles, providing convenient handles for subsequent synthetic elaboration (**30, 47, 48, 50–53**). A noticeable limitation of the scope was observed: electron-rich sulfonyl hydrazones yielded only traces of the desired product, with a notable reduction of the carboxylic acid. Additionally, under slightly modified reaction conditions (see Supplementary Table 7), unactivated aliphatic aldehyde-derived sulfonyl hydrazones acted as effective coupling partners, delivering alkylated secondary amines in

synthetically useful yields, and underlining the method's simplicity and versatility (**54–58**).

#### Late-stage modification of peptides on solid phase

Having demonstrated the generality of the photochemical cross-electrophile coupling between sulfonyl hydrazones and RAEs, we turned our inquiry toward the potential extension of this protocol to facilitate the late-stage functionalization (LSF) of more complex molecules, such as peptides. Given the increasing prominence of peptides as therapeutic modalities, the development of methods capable of functionalizing extensive amino acid sequences directly on resin becomes especially valuable, enabling the generation of diversity without necessitating the development of de-novo synthetic methods<sup>37,38</sup>. Moreover, on-resin modification brings forth substantial practical advantages, addressing key challenges related to purification and solubility that are often encountered in peptide chemistry in solution. Specifically, considering the well-documented compatibility

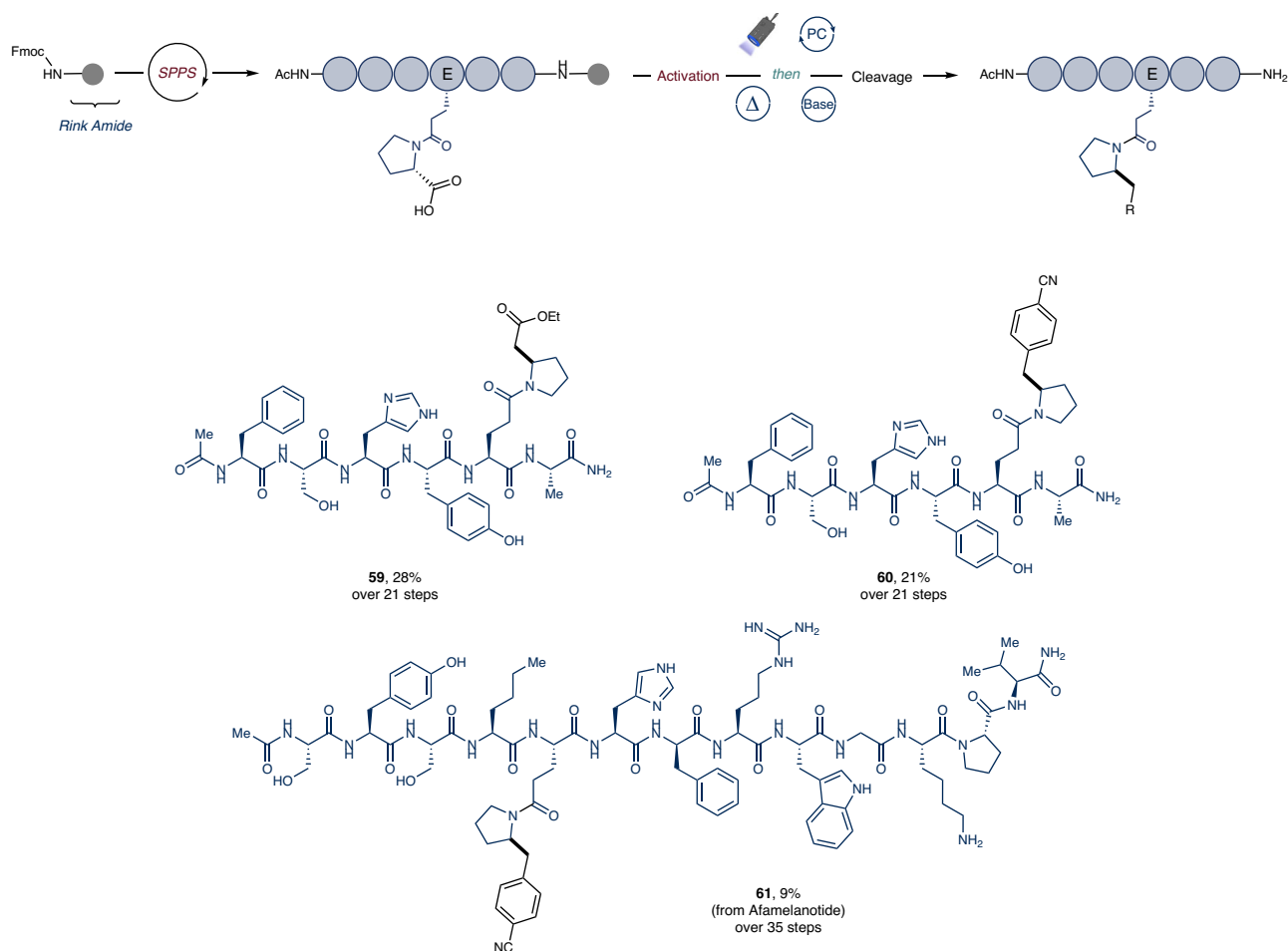


**Fig. 4 | Scope of the cross-electrophile coupling of peptide RAEs on resin.** Reaction conditions: RAE (0.03 mmol, 1 equiv.), Sulfonyl Hydrazine (3 equiv.), Hantzsch ester (4.5 equiv.) and EYNa<sub>2</sub> (0.30 equiv.) in CH<sub>2</sub>Cl<sub>2</sub> (33 mM). For full experimental details, see the Supplementary Information.

of redox-active ester synthesis with solid-phase approaches<sup>47,59,60</sup>, and the mild basic condition of our two-step protocol, we hypothesized that adapting this photochemical transformation to heterogeneous conditions on resin would be an attainable objective.

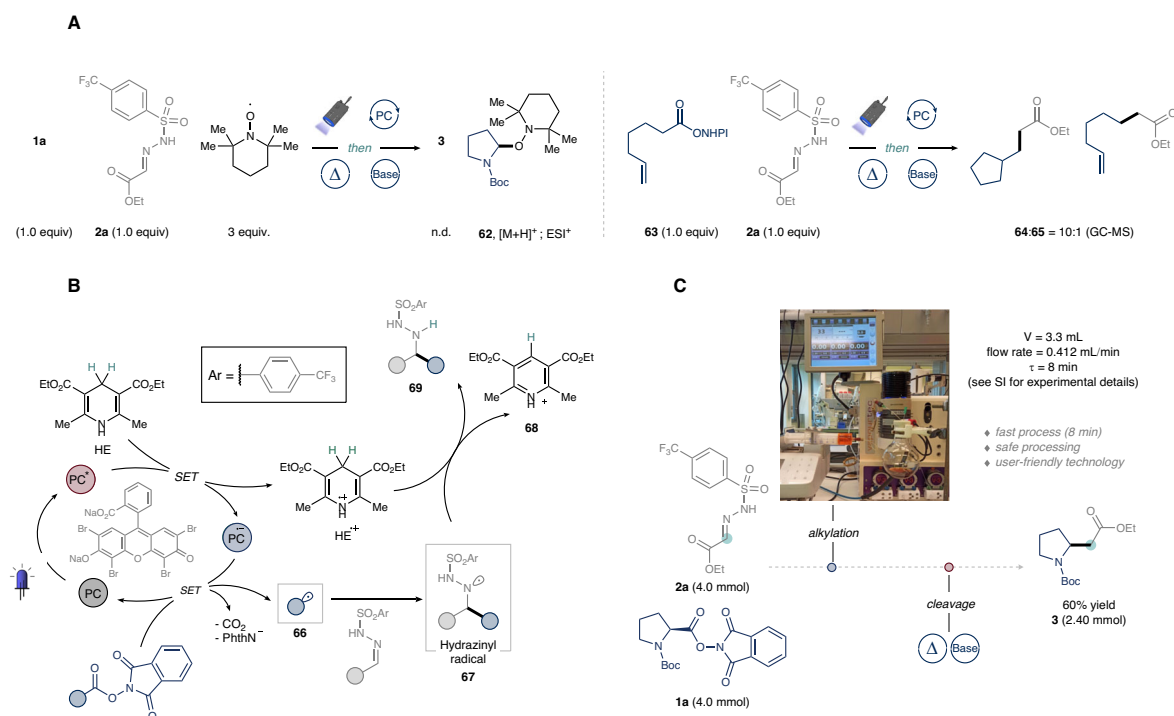
At the outset of our investigation, a sensitivity/robustness screening was undertaken to determine which amino acids would be compatible with our reaction conditions and, consequently, could be possibly incorporated into the peptide sequence (see Supplementary Information, Section 5.4). Pleasingly, all screened amino acid residues, when added as additives, did not interfere with the model reaction. Following a minor re-optimization of the reaction parameters and modification of the experimental setup (see Supplementary Information, Sections 7.1–7.4), we discovered that crude peptides, synthesized using Rink Amide resin via SPPS, could be readily engaged in the photocatalytic alkylation (Fig. 4). Illustratively, heptapeptide **P1** was subjected to LSF, yielding the corresponding homoproline-containing analogue **59** in a 28% isolated yield after 21 steps from resin loading (74% LCAP for the decarboxylative alkylation step, with LCAP defined as LC Area % of the product peak in the ultra-performance liquid chromatography (UPLC) chromatogram of the reaction crude. See Supplementary Information, Section 7.5, Supplementary Fig. 20). Highlighting the efficacy of our method, a 28% yield robustly demonstrates the potential of our cross-electrophile coupling for synthesizing complex structures with high selectivity and notable yield conservation. Similarly, a late-stage incorporation of a benzylic unit was accomplished efficiently, demonstrating utility in the context of lipophilicity modulation (**60**) (72% LCAP for the decarboxylative

alkylation step, See Supplementary Information, Section 7.5, Supplementary Fig. 22). To our delight, a derivative of afamelanotide—a therapeutic peptide indicated for patients affected by erythropoietic protoporphyria—was also successfully engaged in the protocol, affording derivative **61** in an overall 9% yield from resin loading (71% LCAP for the decarboxylative alkylation step. See Supplementary Information, Section 7.5, Supplementary Fig. 24)<sup>61</sup>.

### Mechanistic investigations

In our pursuit to elucidate the mechanism, we executed a series of experiments to explore the radical pathway and identify the catalytic species facilitating the photochemical transformation. Confirmation of the radical nature of the reaction was achieved through radical trapping and radical clock experiments (Fig. 5A)<sup>62</sup>. Indeed, ESI-HRMS analysis substantiated the formation of TEMPO adduct **62**, while GC-MS analysis convincingly demonstrated carbon radical formation through the production of **64** via a 5-exo-trig radical cyclization.

In light of these observations and based on the reported Single Electron Transfer (SET) mechanism of EYNa<sub>2</sub>, we propose the ensuing catalytic cycle (see Fig. 5B)<sup>63,64</sup>. Upon absorption of visible light, the triplet excited state of EYNa<sub>2</sub> is reductively quenched by the sacrificial electron donor HE to generate HE<sup>+</sup>. Following the findings of Overmann and König<sup>65–67</sup>, the redox-active ester is subsequently reduced by the EYNa<sub>2</sub> radical anion, thereby completing the catalytic cycle and yielding the nucleophilic alkyl radical **66** upon decarboxylation. The emergent alkyl radical is then captured by the electrophilic site of sulfonyl hydrazine, resulting in the formation of the hydrazinyl radical



intermediate **67**. Finally, a plausible Hydrogen Atom Transfer (HAT) step from  $\text{HE}^+$  or neutral  $\text{HE}$  to **67** is considered, generating the pyridium co-product **68** and the targeted product **69**.

### Scale up

Finally, we demonstrate the scalability of our photochemical C1 homologation using flow technology (Fig. 5C). In batch settings above 1 mmol, the heterogeneous reaction mixture led to a significant drop in yield of the desired product **3** (see Supplementary Information, Section 9.1). Suspecting non-uniform irradiation and limited light penetration at larger scales, we transitioned the photochemical alkylative step to continuous flow<sup>68–70</sup>. After an extensive optimization conducted at 0.2 mmol scale (see Supplementary Information, Section 9.2), we established conditions for the protocol using a Vapourtec UV-150 photochemical flow reactor (ID: 0.8 mm;  $V = 3.33$  mL, flow rate =  $0.412$  mL  $\text{min}^{-1}$ ,  $\tau = 8$  min) set at  $30^\circ\text{C}$ , irradiated with 60 W 450 nm LEDs. Subsequent thermal cleavage of the alkylated hydrazide intermediate yielded the targeted C1 homologated product in 60% isolated yield.

### Discussion

In summary, we have developed a visible light mediated metal-free cross-electrophile coupling approach that stands as a powerful and versatile  $\text{C}(\text{sp}^3)\text{-C}(\text{sp}^3)$  cross-coupling platform. It combines carboxylic acid-derived redox-active esters with aldehyde sulfonyl hydrazones, utilizing Eosin Y as an efficient organophotocatalyst under visible light, leading to the desired cross-coupled products through subsequent fragmentation. Our approach provides a safer alternative to the traditional Arndt-Eistert reaction for C1 homologation of carboxylic acids and enables direct synthesis of cyclic and acyclic  $\beta$ -arylethylamines using diverse aldehyde-derived sulfonyl hydrazones. Furthermore, the method proves also effective for late-stage functionalization (LSF) of peptides on solid-phase. Given these capabilities, we are confident our method will enable the exploration of  $\text{sp}^3$ -hybridized molecules in contemporary drug discovery and development.

### Data availability

The data supporting the results of the article, including optimization studies, experimental procedures, compound characterization, late stage modification of peptides on solid phase, mechanistic studies and scale-up procedures are provided within the paper and its Supplementary Information. Additional data are available from the corresponding author upon request.

### References

- Wei, W., Cherukupalli, S., Jing, L., Liu, X. & Zhan, P. Fsp3: A new parameter for drug-likeness. *Drug Discov. Today* **25**, 1839–1845 (2020).
- Lovering, F., Bikker, J. & Humblet, C. Escape from Flatland: Increasing Saturation as an Approach to Improving Clinical Success. *J. Med. Chem.* **52**, 6752–6756 (2009).
- Clemons, P. A. et al. Small molecules of different origins have distinct distributions of structural complexity that correlate with protein-binding profiles. *Proc. Natl Acad. Sci.* **107**, 18787–18792 (2010).
- Brown, D. G. & Boström, J. Analysis of Past and Present Synthetic Methodologies on Medicinal Chemistry: Where Have All the New Reactions Gone? *J. Med. Chem.* **59**, 4443–4458 (2016).
- Tasker, S. Z., Standley, E. A. & Jamison, T. F. Recent advances in homogeneous nickel catalysis. *Nature* **509**, 299–309 (2014).
- Choi, J. & Fu, G. C. Transition metal-catalyzed alkyl-alkyl bond formation: Another dimension in cross-coupling chemistry. *Science* **356**, eaaf7230 (2017).
- Blakemore, D. C. et al. Organic synthesis provides opportunities to transform drug discovery. *Nat. Chem.* **10**, 383–394 (2018).
- Zhang, B. et al. Ni-electrocatalytic  $\text{Csp}^3\text{-Csp}^3$  doubly decarboxylative coupling. *Nature* **606**, 313–318 (2022).
- Hioki, Y. et al. Overcoming the limitations of Kolbe coupling with waveform-controlled electrosynthesis. *Science* **380**, 81–87 (2023).
- Johnston, C. P., Smith, R. T., Allmendinger, S. & MacMillan, D. W. C. Metallaphotoredox-catalyzed  $\text{sp}^3\text{-sp}^3$  cross-coupling of carboxylic acids with alkyl halides. *Nature* **536**, 322–325 (2016).

- Smith, R. T. et al. Metallaphotoredox-Catalyzed Cross-Electrophile Csp<sup>3</sup>-Csp<sup>3</sup> Coupling of Aliphatic Bromides. *J. Am. Chem. Soc.* **140**, 17433–17438 (2018).
- Liu, W., Lavagnino, M. N., Gould, C. A., Alcázar, J. & MacMillan, D. W. C. A biomimetic S<sub>H</sub>2 cross-coupling mechanism for quaternary sp<sup>3</sup>-carbon formation. *Science* **374**, 1258–1263 (2021).
- Lyon, W. L. & MacMillan, D. W. C. Expedient Access to Underexplored Chemical Space: Deoxygenative C(sp<sup>3</sup>)-C(sp<sup>3</sup>) Cross-Coupling. *J. Am. Chem. Soc.* **145**, 7736–7742 (2023).
- Kang, K. & Weix, D. J. Nickel-Catalyzed C(sp<sup>3</sup>)-C(sp<sup>3</sup>) Cross-Electrophile Coupling of In Situ Generated NHP Esters with Unactivated Alkyl Bromides. *Org. Lett.* **24**, 2853–2857 (2022).
- Douthwaite, J. L. et al. Formal Cross-Coupling of Amines and Carboxylic Acids to Form sp<sup>3</sup>-sp<sup>2</sup> Carbon-Carbon Bonds. *J. Am. Chem. Soc.* **145**, 10930–10937 (2023).
- Sakai, H. A. & MacMillan, D. W. C. Nontraditional Fragment Couplings of Alcohols and Carboxylic Acids: C(sp<sup>3</sup>)-C(sp<sup>3</sup>) Cross-Coupling via Radical Sorting. *J. Am. Chem. Soc.* **144**, 6185–6192 (2022).
- Xiao, J., Li, Z. & Montgomery, J. Nickel-Catalyzed Decarboxylative Coupling of Redox-Active Esters with Aliphatic Aldehydes. *J. Am. Chem. Soc.* **143**, 21234–21240 (2021).
- Gao, Y. et al. Electrochemical Nozaki-Hiyama-Kishi Coupling: Scope, Applications, and Mechanism. *J. Am. Chem. Soc.* **143**, 9478–9488 (2021).
- Yang, Y. et al. Practical and Modular Construction of C(sp<sup>3</sup>)-Rich Alkyl Boron Compounds. *J. Am. Chem. Soc.* **143**, 471–480 (2021).
- Liu, Z. et al. Silver-catalyzed site-selective C(sp<sup>3</sup>)-H benzylation of ethers with N-trifosylhydrazones. *Nat. Commun.* **13**, 1674 (2022).
- Wang, H., Wang, S., George, V., Llorente, G. & König, B. Photo-Induced Homologation of Carbonyl Compounds for Iterative Syntheses. *Angew. Chem. Int. Ed.* **61**, e202211578 (2022).
- Dao, H. T., Li, C., Michaudel, Q., Maxwell, B. D. & Baran, P. S. Hydromethylation of Unactivated. *Olefin J. Am. Chem. Soc.* **137**, 8046–8049 (2015).
- Saladrigas, M., Bonjoch, J. & Bradshaw, B. Iron hydride radical reductive alkylation of unactivated alkenes. *Org. Lett.* **22**, 684–688 (2020).
- Kim, S. Radical cyclization involving the evolution of nitrogen. *Pure Appl. Chem.* **68**, 623–626 (1996).
- Wang, S., Cheng, B.-Y., Sršen, M. & König, B. Umpolung Difunctionalization of Carbonyls via Visible-Light Photoredox Catalytic Radical-Carbanion Relay. *J. Am. Chem. Soc.* **142**, 7524–7531 (2020).
- Kinsella, A. G., Tibbetts, J. D., Stead, D. & Cresswell, A. J. N-tosylhydrazones as acceptors for nucleophilic alkyl radicals in photoredox catalysis: A short case study on possible side reactions. *Synth. Commun.* **52**, 413–423 (2022).
- Pulcinella, A., Bonciolini, S., Lukas, F., Sorato, A. & Noël, T. Photocatalytic Alkylation of C(sp<sup>3</sup>)-H Bonds Using Sulfonylhydrazones. *Angew. Chem. Int. Ed.* **62**, e202215374 (2023).
- Merchant, R. R. & Lopez, J. A. A General C(sp<sup>3</sup>)-C(sp<sup>3</sup>) Cross-Coupling of Benzyl Sulfonylhydrazones with Alkyl Boronic Acids. *Org. Lett.* **22**, 2271–2275 (2020).
- Okada, K., Okamoto, K. & Oda, M. A new and practical method of decarboxylation: photosensitized decarboxylation of N-acyloxyphthalimides via electron-transfer mechanism. *J. Am. Chem. Soc.* **110**, 8736–8738 (1988).
- Okada, K., Okamoto, K., Morita, N., Okubo, K. & Oda, M. Photosensitized decarboxylative Michael addition through N-(acyloxy)phthalimides via an electron-transfer mechanism. *J. Am. Chem. Soc.* **113**, 9401–9402 (1991).
- Parida, S. K. et al. Single Electron Transfer-Induced Redox Processes Involving N-(Acyloxy)phthalimides. *ACS Catal.* **11**, 1640–1683 (2021).
- Murarka, S. N-(Acyloxy)phthalimides as Redox-Active Esters in Cross-Coupling Reactions. *Adv. Synth. Catal.* **360**, 1735–1753 (2018).
- Noël, T. & Zysman-Colman, E. The promise and pitfalls of photocatalysis for organic synthesis. *Chem. Catal.* **2**, 468–476 (2022).
- Podlech, J. & Seebach, D. The Arndt-Eistert Reaction in Peptide Chemistry: A Facile Access to Homopeptides. *Angew. Chem. Int. Ed. Engl.* **34**, 471–472 (1995).
- Winum, J.-Y., Kamal, M., Leydet, A., Roque, J.-P. & Montero, J.-L. Homologation of carboxylic acids by arndt-eistert reaction under ultrasonic waves. *Tetrahedron Lett.* **37**, 1781–1782 (1996).
- Marti, R. E., Bleicher, K. H. & Bair, K. W. Solid Phase Synthesis of β-Peptides via Arndt-Eistert Homologation of Fmoc-Protected Amino Acid Diazoketones. *Tetrahedron Lett.* **38**, 6145–6148 (1997).
- Bernardim, B., Hardman-Baldwin, A. M. & Burtoloso, A. C. B. LED lighting as a simple, inexpensive, and sustainable alternative for Wolff rearrangements. *RSC Adv.* **5**, 13311–13314 (2015).
- Mastronardi, F., Gutmann, B. & Oliver Kappe, C. Continuous flow generation and reactions of anhydrous diazomethane using a teflon AF-2400 tube-in-tube reactor. *Org. Lett.* **15**, 5590–5593 (2013).
- Katritzky, A. R., Zhang, S. & Fang, Y. BtCH<sub>2</sub>TMS-Assisted Homologation of Carboxylic Acids: A Safe Alternative to the Arndt-Eistert Reaction. *Org. Lett.* **2**, 3789–3791 (2000).
- Kowalski, C. J., Haque, M. S. & Fields, K. W. Ester homologation via α-bromo α-keto dianion rearrangement. *J. Am. Chem. Soc.* **107**, 1429–1430 (1985).
- Kowalski, C. J. & Reddy, R. E. Ester homologation revisited: a reliable, higher yielding and better understood procedure. *J. Org. Chem.* **57**, 7194–7208 (1992).
- Derek, H. R., Barton Ching-Yuh, C. & Joseph, J. C. Homologation of acids via carbon radicals generated from the acyl derivatives of N-hydroxy-2-thiopyridone. (The two-carbon problem). *Tetrahedron Lett.* **32**, 3309–3312 (1991).
- Barton, D. H. R., Ching-Yuh, C. & Jaszberenyi, J. C. Homologation of carboxylic acids by improved methods based on radical chain chemistry of acyl derivatives of N-hydroxy-2-thiopyridone. *Tetrahedron Lett.* **33**, 5013–5016 (1992).
- Pozhydaev, V., Muller, C., Moran, J. & Lebœuf, D. Catalytic Synthesis of β-(Hetero)arylethylamines: Modern Strategies and Advances. *Angew. Chem. Int. Ed.* **62**, e202309289 (2023).
- Bunescu, A., Abdelhamid, Y. & Gaunt, M. J. Multicomponent alkene azidoarylation by anion-mediated dual catalysis. *Nature* **598**, 597–603 (2021).
- Noten, E. A., McAtee, R. C. & Stephenson, C. R. J. Catalytic intramolecular aminoarylation of unactivated alkenes with aryl sulfonamides. *Chem. Sci.* **13**, 6942–6949 (2022).
- Qin, T. et al. A general alkyl-alkyl cross-coupling enabled by redox-active esters and alkylzinc reagents. *Science* **352**, 801–805 (2016).
- Noisier, A. F. M. et al. Late-Stage Functionalization of Histidine in Unprotected Peptides. *Angew. Chem. Int. Ed.* **58**, 19096–19102 (2019).
- Twitty, J. C. et al. Diversifying Amino Acids and Peptides via Deaminative Reductive Cross-Couplings Leveraging High-Throughput Experimentation. *J. Am. Chem. Soc.* **145**, 5684–5695 (2023).
- Barluenga, J., Tomás-Gamasa, M., Aznar, F. & Valdés, C. Metal-free carbon-carbon bond-forming reductive coupling between boronic acids and tosylhydrazones. *Nat. Chem.* **1**, 494–499 (2009).
- Prier, C. K., Rankic, D. A. & MacMillan, D. W. C. Visible Light Photoredox Catalysis with Transition Metal Complexes: Applications in Organic Synthesis. *Chem. Rev.* **113**, 5322–5363 (2013).
- Romero, N. A. & Nicewicz, D. A. Organic Photoredox Catalysis. *Chem. Rev.* **116**, 10075–10166 (2016).
- Kammer, L. M., Badir, S. O., Hu, R.-M. & Molander, G. A. Photoactive electron donor-acceptor complex platform for Ni-mediated C(sp<sup>3</sup>)-C(sp<sup>2</sup>) bond formation. *Chem. Sci.* **12**, 5450–5457 (2021).



54. Crisenza, G. E. M., Mazzarella, D. & Melchiorre, P. Synthetic Methods Driven by the Photoactivity of Electron Donor–Acceptor Complexes. *J. Am. Chem. Soc.* **142**, 5461–5476 (2020).
55. Zhang, Y., Yin, Z. & Wu, X.-F. Copper-Catalyzed Carbonylative Synthesis of  $\beta$ -Homoprolines from *N*-Fluoro-sulfonamides. *Org. Lett.* **22**, 1889–1893 (2020).
56. Vitaku, E., Smith, D. T. & Njardarson, J. T. Analysis of the Structural Diversity, Substitution Patterns, and Frequency of Nitrogen Heterocycles among U.S. FDA Approved Pharmaceuticals. *J. Med. Chem.* **57**, 10257–10274 (2014).
57. White, A. M., Palombi, I. R. & Malins, L. R. Umpolung strategies for the functionalization of peptides and proteins. *Chem. Sci.* **13**, 2809–2823 (2022).
58. Mackay, A. S., Payne, R. J. & Malins, L. R. Electrochemistry for the Chemoselective Modification of Peptides and Proteins. *J. Am. Chem. Soc.* **144**, 23–41 (2022).
59. Qin, T. et al. Nickel-Catalyzed Barton Decarboxylation and Giese Reactions: A Practical Take on Classic Transforms. *Angew. Chem. Int. Ed.* **129**, 266–271 (2017).
60. Pal, S., Openy, J., Krzyzanowski, A., Noisier, A. & Hart, P. On-Resin Photochemical Decarboxylative Arylation of Peptides. *Org. Lett.* <https://doi.org/10.1021/acs.orglett.3c03070> (2023).
61. Langendonk, J. G. et al. Afamelanotide for Erythropoietic Protoporphyrria. *N. Engl. J. Med.* **373**, 48–59 (2015).
62. Buzzetti, L., Crisenza, G. E. M. & Melchiorre, P. Mechanistic Studies in Photocatalysis. *Angew. Chem. Int. Ed.* **58**, 3730–3747 (2019).
63. Xu, R., Xu, T., Yang, M., Cao, T. & Liao, S. A rapid access to aliphatic sulfonyl fluorides. *Nat. Commun.* **10**, 3752 (2019).
64. Zhang, M., Yu, M., Wang, Z., Liu, Y. & Wang, Q. Rapid Access to Aliphatic Sulfonamides. *Org. Lett.* **24**, 3932–3937 (2022).
65. Pratsch, G., Lackner, G. L. & Overman, L. E. Constructing Quaternary Carbons from *N*-(Acyloxy)phthalimide Precursors of Tertiary Radicals Using Visible-Light Photocatalysis. *J. Org. Chem.* **80**, 6025–6036 (2015).
66. Lackner, G. L., Quasdorf, K. W., Pratsch, G. & Overman, L. E. Fragment Coupling and the Construction of Quaternary Carbons Using Tertiary Radicals Generated from *tert*-Alkyl *N*-Phthalimidoyl Oxalates by Visible-Light Photocatalysis. *J. Org. Chem.* **80**, 6012–6024 (2015).
67. Schwarz, J. & König, B. Metal-free, visible-light-mediated, decarboxylative alkylation of biomass-derived compounds. *Green. Chem.* **18**, 4743–4749 (2016).
68. Capaldo, L., Wen, Z. & Noël, T. A field guide to flow chemistry for synthetic organic chemists. *Chem. Sci.* **14**, 4230–4247 (2023).
69. Capaldo, L., Bonciolini, S., Pulcinella, A., Nuño, M. & Noël, T. Modular allylation of  $C(sp^3)$ -H bonds by combining decatungstate photocatalysis and HWE olefination in flow. *Chem. Sci.* **13**, 7325–7331 (2022).
70. Mazzarella, D., Pulcinella, A., Bovy, L., Broersma, R. & Noël, T. Rapid and Direct Photocatalytic  $C(sp^3)$ -H Acylation and Arylation in Flow. *Angew. Chem. Int. Ed.* **60**, 21277–21282 (2021).

## Acknowledgements

We are grateful to have received generous funding from the European Union H2020 research and innovation program under the Marie S. Curie Grant Agreement (PhotoReAct, No 956324, S.B., M.L., A.L., G.M., E.Z.C., T.N.; CHAIR, No 860762, A.P., M.J., T.N.). We also would like to thank Ed Zuidinga for help with the HRMS measurements.

## Author contributions

S.B. and A.P. designed the project, with input from T.N. S.B., A.P., M.L., D.S., A.L.R., A.S. performed and analyzed the synthetic experiments with input from G.M., N.D.C. and T.N. The peptide work was carried out by A.P. and was supervised by M.J., M.A.J.D. and R.G. The mechanistic studies were carried out by S.B., and supervised by E.Z.C., S.P., M.F. and T.N. The flow studies were carried out by S.B. and A.P. and supervised by T.N. All authors provided input during the progress meetings. S.B., A.P. and T.N. wrote the manuscript with input from all the authors.

## Competing interests

The authors declare no competing interest.

## Additional information

**Supplementary information** The online version contains supplementary material available at <https://doi.org/10.1038/s41467-024-45804-z>.

**Correspondence** and requests for materials should be addressed to Timothy Noël.

**Peer review information** *Nature Communications* thanks Wei Shu and the other, anonymous, reviewer(s) for their contribution to the peer review of this work. A peer review file is available.

**Reprints and permissions information** is available at <http://www.nature.com/reprints>

**Publisher's note** Springer Nature remains neutral with regard to jurisdictional claims in published maps and institutional affiliations.

**Open Access** This article is licensed under a Creative Commons Attribution 4.0 International License, which permits use, sharing, adaptation, distribution and reproduction in any medium or format, as long as you give appropriate credit to the original author(s) and the source, provide a link to the Creative Commons licence, and indicate if changes were made. The images or other third party material in this article are included in the article's Creative Commons licence, unless indicated otherwise in a credit line to the material. If material is not included in the article's Creative Commons licence and your intended use is not permitted by statutory regulation or exceeds the permitted use, you will need to obtain permission directly from the copyright holder. To view a copy of this licence, visit <http://creativecommons.org/licenses/by/4.0/>.

© The Author(s) 2024